PHYSICAL REVIEW D VOLUME 20, NUMBER 7 1 OCTOBER 1979

Charged-particle multiplicity distributions in *pd* and *pn* interactions at 400 GeV/*c*

S. Dado,* S. J. Barish, A. Engler, and R. W. Kraemer
Carnegie-Mellon University, Pittsburgh, Pennsylvania 15213

J. E. A. Lys† and C. T. Murphy
Fermi National Accelerator Laboratory, Batavia, Illinois 60510

A. Brody,‡ J. Hanlon, T. Kafka, F. Lo Pinto, and S. Sommars
State University of New York at Stony Brook, Stony Brook, New York 11794

(Received 26 February 1979)

Charged-particle multiplicity distributions in 400-GeV/*c* *pd* interactions have been studied in an experiment in the Fermilab 30-inch bubble chamber. From the fractions of odd-prong and backward-proton events, a rescatter fraction of 0.22 ± 0.01 is found (for $N \geq 3$). The *pn* multiplicity distribution is obtained from the odd-prong distribution plus a no-cascade assumption. After making one-prong and two-prong estimates, mean charged-particle multiplicities of 9.49 ± 0.12 for *pd* (including slow particles) and 8.57 ± 0.12 for *pn* are obtained. In the incident momentum range 100 to 400 GeV/*c*, *pd* and *pp* distributions are very similar to each other and are different from *pn* distributions.

INTRODUCTION

This paper presents results on charged-particle multiplicity distributions from a proton-deuteron experiment at an incident momentum of 400 GeV/*c*. Properties of the *pd* multiplicity distribution and of the derived *pn* multiplicity distribution are compared to those found at lower energies and to those for *pp* interactions. The fraction of events in which rescattering occurs is determined and is compared to that found in other deuteron experiments.

MEASUREMENT OF MULTIPLICITY DISTRIBUTIONS

The present data come from 51 000 pictures of the Fermilab 30-inch deuterium-filled bubble chamber exposed to a beam of 400-GeV/*c* protons. Since the primary beam momentum was 400 GeV/*c*, we expect negligible beam contamination by nonproton particles.

The film was scanned twice for all interactions with three or more outgoing charged particles (prongs) produced by beam tracks in a 45-cm-long fiducial volume. Pictures in which more than 12 beam tracks or more than a total of 20 tracks entered the fiducial volume were rejected. The combined scanning efficiency was $(99 \pm 1)\%$, independent of multiplicity. The number of prongs was counted for each event on each scan; the prong count included any short visible proton or deuteron tracks. Odd-prong events, in which there is presumably an unobservable short proton or deuteron track, constituted 27% of the scanned events. All events with prong-count discrepancies between the two scans were examined by a physicist or a third scanner who made a final prong-count decision.

Approximately 9% of the events were assigned to an uncountable category. More uncountable events are expected at this high beam energy than at lower energies because of the higher mean multiplicity and the greater collimation of the produced particles. The problem is worse in deuterium than in hydrogen, since in the former both odd- and even-prong counts are allowed, and it is important to separate odd-prong events from even-prong events. Most of the uncountable events had either a confusing secondary interaction downstream from the primary vertex or had two or more tracks that overlapped in all three views for their entire path in the bubble chamber. Most of the scanning was done with a magnification that gave a 1.3-times-life-size image. A reexamination of some uncountable events with a 3-times-life-size image showed that increased magnification could not resolve uncountable events.

The contribution of the uncountable events to the multiplicity distribution was estimated as follows. For each such event a minimum and a maximum primary-vertex prong count was determined at the scanning table, thus defining an allowed range of prong counts. Then the event was assumed to make a fractional contribution to each prong count in its allowed range of f_0/n_0 for odd-prong counts and $(1-f_0)/n_e$ for even-prong counts. Here f_0 is the fraction of odd-prong events in the countable events, $f_0 \approx 0.27$, and n_0 and n_e are, respectively, the numbers of odd- and even-prong counts in the allowed range. The mean value of the difference between the minimum and maximum prong counts was 3.1 units.

Uncertainty in how to assign the uncountable events leads to systematic errors in the multip-

TABLE I. Odd-prong multiplicity distributions (after 5-mm range cut, see text).

Prong count	Countable events	Uncountable events	Corrected total [a]
3	888	27	930 ± 32
5	942	54	1005 ± 34
7	1010	77	1100 ± 34
9	945	83	1037 ± 33
11	761	84	835 ± 30
13	511	65	553 ± 25
15	351	57	387 ± 21
17	204	45	227 ± 17
19	101	37	118 ± 14
21	61	21	70 ± 11
23	16	11	15 ± 7
25	13	6	14 ± 5
27	5	2	3 ± 3
29	1	0	1 ± 1
Total	5809	569	6295

[a] Errors are partly correlated via systematic errors in uncountable event assignment.

licity distributions and their moments. These systematic errors were estimated as follows. For any quantity F, two values were determined, corresponding to two possible methods of assigning the uncountable events: (a) the method described above, and (b) an extreme method of assigning the minimum value in the allowed range (with an appropriate adjustment if considering the odd-prongs). The difference between the two values of F is a measure of the maximum possible error, and a systematic error of one-half this difference was then assumed. Systematic and statistical errors were combined in quadrature. For all quantities given in this paper, the systematic error was less than the statistical error.

The multiplicity distributions for the countable events and for the uncountable events distributed as described above (with fractions rounded off) are given in Table I for odd-prong counts and in Table II for even- plus odd-prong counts. In the latter, one is always added to odd-prong counts to take account of the presumed invisible proton or deuteron present. All odd-prong numbers in Table I include the short proton visibility correction detailed below.

In order to arrive at final multiplicity distributions, several corrections must be considered. These are detailed below.

Short proton visibility. It may be expected that very short proton (or deuteron) tracks are easier to detect in low-multiplicity events than in high-multiplicity events. Therefore, all even-prong events with a stopping track of length less than 5 mm in space were added to the next lower odd-prong category. The cut at 5 mm, which was implemented using measurements of the events, corresponds to a momentum cut at 120 MeV/c for protons. Thus the odd-prong distributions in this

TABLE II. Even- plus odd-prong multiplicity distributions.

Prong count	Countable events	Uncountable events	Corrected total [a]	Cross section (mb)	Backward proton events [b]
4	2 383	108	2 518 ± 62	7.70 ± 0.22	90 ± 11
6	2 706	198	2 941 ± 66	8.99 ± 0.24	97 ± 11
8	2 954	244	3 245 ± 60	9.92 ± 0.23	97 ± 11
10	2 742	266	3 056 ± 57	9.34 ± 0.22	94 ± 11
12	2 208	251	2 460 ± 51	7.52 ± 0.19	79 ± 11
14	1 514	204	1 685 ± 45	5.15 ± 0.16	48 ± 8
16	1 012	165	1 148 ± 37	3.51 ± 0.12	27 ± 6
18	579	131	674 ± 31	2.06 ± 0.10	15 ± 5
20	330	98	399 ± 29	1.22 ± 0.09	7 ± 4
22	187	58	224 ± 22	0.68 ± 0.07	3 ± 2
24	87	32	102 ± 15	0.31 ± 0.05	2 ± 2
26	54	17	63 ± 10	0.19 ± 0.03	3 ± 2
28	20	8	21 ± 6	0.064 ± 0.018	0
30	6	1	5 ± 3	0.015 ± 0.009	0
32	4	1	6 ± 2	0.018 ± 0.006	0
34	0	0	0	0	0
36	1	0	1 ± 1	0.003 ± 0.003	0
Total	16 787	1782	18 548	56.7 ± 0.8	562

[a] See footnote a of Table I.
[b] Even-prong events with a backward proton with momentum >120 MeV/c.

paper refer to events in which one charged particle has a range of less than 5 mm. The mean multiplicity of the resulting odd-prong distribution was 0.15 units lower than that for the uncorrected distribution. This correction does not apply to the even- plus odd-prong distribution (Table II), where even invisibly short tracks are included in the count.

Unobserved Dalitz pairs. A fit[1] to pp data indicates that at 400 GeV/c the mean number of π^0 per inelastic pp interaction is 3.9. Assuming the same mean for 400-GeV/c pd events, it was found that 72% of Dalitz pairs were not observed in the scanning. The multiplicity distributions were then corrected appropriately, assuming the same multiplicity dependence for π^0 production as found for 300-GeV/c pp interactions.[2] This correction reduced the mean multiplicity for both odd-prong and even- plus odd-prong distributions by 0.06 units.

Unobserved vees. For a sample of events, a histogram was made of the distance on the scanning table of the nearest neutral particle decay or gamma conversion (vee) from the primary vertex. From a study of this histogram it was concluded that approximately 60% of the vees that occurred within 1.5 cm of the primary vertex were incorrectly included in the primary-vertex prong count, equivalent to a loss of 180 vees in the total event sample. The resulting correction, which assumed the same multiplicity dependence for Λ, K_S^0 and π^0 production as for 300-GeV/c pp interactions,[2] reduced the mean multiplicities by 0.02 units.

Unobserved close secondaries. A histogram of the distance on the scanning table from the primary vertex to the nearest secondary vertex indicated a loss of 50% of secondary interactions within 1 cm of the primary vertex. In making corrections for this loss, the observed-secondary-interaction prong-count distribution was used. Since 80% of the observed secondary interactions have an even-prong count (51% are two-prong interactions), the result of an unobserved secondary is generally to change an odd-prong event into an apparent even-prong event, or vice versa. The resulting mean multiplicity reduction was 0.12 units for the odd-prong distribution and 0.03 units for the even- plus odd-prong distribution.

The final corrected multiplicity distributions are given in column 4 of Tables I and II. It is worth emphasizing that the numbers in Table I are intended to represent events that have an odd primary vertex prong count after any protons or deuterons with a range of less than 5 mm in the bubble chamber are removed from the prong count. For completeness, column 6 of Table II gives the corrected multiplicity distribution of even-prong events that have a proton that is backwards in the laboratory and has momentum >120 MeV/c.

Cross sections. A sample of 44 000 pictures was used to measure the cross section for events with three or more prongs. On 33 236 acceptable pictures in this sample 16 341 such events were found in the fiducial volume with acceptable beam tracks. The cross section was calculated to be 56.7± 0.8 mb. The target density was determined to be 0.1364± 0.0007 g/cm^3 from the thermodynamic operating conditions of the bubble chamber.

The above cross section may be compared with values found at[3] 100 and[4] 200 GeV/c of 54.0± 2.0 mb and 55.05± 0.78 mb, respectively, both for pd interactions with three or more prongs.

The resulting topological cross sections for the even- plus odd-prongs events are given in column 5 of Table II.

RESCATTER FRACTION

The fraction F_{rs} of rescatter events has been calculated in the same manner[5] as at 100 GeV/c. Here a rescatter event is taken to mean one in which both nucleons in the deuteron take an active part, as opposed to events in which one nucleon can be considered as a spectator. The fraction considered here is always for events with three or more prongs ($N \geq 3$).

The following formulas were used to calculate F_{rs}:

$$F_{rs} = 1 - \frac{M(p_s) + M(n_s)}{M(\text{tot})}, \tag{1a}$$

$$M(p_s) = M(\text{odd}) + (1+r)M(\text{back } p), \tag{1b}$$

$$M(n_s) = M(p_s)\sigma(pp, N \geq 4)/\sigma(pn, N \geq 3). \tag{1c}$$

Here M denotes numbers of events, $M(p_s)$ and $M(n_s)$ are the numbers of events with a spectator proton and a spectator neutron, respectively, and $M(\text{back } p)$ is the number of even-prong events with a proton that is backwards in the laboratory. The quantity r equals the ratio of the number of visible spectator protons that go forward in the laboratory (i.e., have angle <90° with respect to the beam direction) to the number that go backwards. If we assume that r differs from unity solely through the Moller flux factor, then from the backward protons in this experiment (with momentum >120 MeV/c) we obtain $r = 1.25 \pm 0.01$. This is the value we use below. At 100 GeV/c it was found[5,6] that if elastic rescattering was taken into account the value of r could increase by ~0.16; in the present experiment such an increase would decrease the value obtained for F_{rs} by 0.010.

To determine the cross-section ratio in Eq. (1c), it was assumed that at 400 GeV/c the pp and pn total inelastic cross sections are equal, with an error of ±2%, and that the pn one-prong inelastic cross section is given by the same relation as used at[7] 100 GeV/c:

$$\sigma(pn, N=1) = (0.6 \pm 0.1)\sigma(pp, N=2)\,. \quad (2)$$

The two-prong inelastic pp cross section at 400 GeV/c was taken from Ref. 8. The resulting cross section ratio was 0.966± 0.021. Deuteron-final-state events were excluded from M(odd) and M(tot), and neuteron-spectator events were excluded from M(odd) and M(back p); however, the result is rather insensitive to these exclusions. The deuteron-final-state cross sections were estimated as 0.9± 0.2 mb ($N=4$) and 0.2± 0.1 mb ($N=6$), the same values as at[5] 100 GeV/c since measurements[9,10] suggest very little energy dependence. The fractions of neutron-spectator events that enter the odd-prong and backward-proton samples were both taken to be 0.002± 0.001.

The corrected numbers of events used in evaluating F_{rs} were 6005± 97 for M(odd), 544± 28 for M(back p), and 18189± 148 for M(tot); the errors are correlated. For M(odd) and M(back p) the 5-mm visibility cut on short tracks is in effect. The result is $F_{rs} = 0.219 \pm 0.013$. The statistical errors and the error in the cross-section ratio contribute approximately equally to the error in F_{rs}.

The above value for F_{rs} can be compared to values of 0.208 + 0.019 at[5] 100 GeV/c and 0.174 ± 0.018 at[4] 200 GeV/c from pd experiments and values close to 0.15 for three πd experiments.[5,11,12] It has been pointed out previously[5] that in hadron-deuteron experiments above ~20 GeV/c, the rescatter fraction appears to be independent of beam energy and to be larger for incident protons than for incident pions. These observations are supported by the present experiment.

ENERGY DEPENDENCE OF pd MULTIPLICITY DISTRIBUTIONS

In this section the 400-GeV/c pd multiplicity distribution is compared with the distributions found at neighboring energies.[4,7,13,14] In the distributions to be discussed, all pd events in which particle production occurs are included, while elastic and quasielastic scatters are excluded. For multiplicities $N \geq 3$, the even- plus odd-prong data are appropriate. However, no high-energy bubble-chamber experiment has measured the relevant $N=2$ contribution because of the difficulty in detecting one-prong events and the difficulty in separating quasielastic events from particle production events—for example, $pd \to ppn$ events from $pd \to ppn\pi^0$ events. Hence an estimate for $N=2$ must be made. For this paper the following assumption is made:

$$P(pd, N=2) = 0.5[P(pn, N=1) + P(pp, N=2)]\,. \quad (3)$$

Here $P(pX, N=i)$ is the probability of an i-prong inelastic collision:

$$P(pX, N=i) = \sigma(pX, N=i)/\sigma(pX, \text{inel})\,.$$

Equation (3) would be correct if the bubble-chamber liquid was comprised of an unbound sea of protons and neutrons in equal numbers and with equal cross sections. We expect that rescattering in the deuteron will cause a decrease in $P(pd, N=2)$ from that given by Eq. (3), while coherent effects may produce an increase. Use of a more complicated formula[15] that attempts to take rescattering and coherent effects[16] into account leads to the same answers within the errors.

In evaluating $P(pd, N=2)$, values of $\sigma(pn, N=1)$ were estimated from pp data and Eq. (2), and the inelastic pn cross section was assumed to be equal to that for pp. The resulting $P(pd, N=2)$ values are included in Table III.

Some properties of the pd multiplicity distributions at 100–400 GeV/c are given in Table III. Also given, for comparison, are pp distribution properties at approximately the same energies.[8,17-22]

In Table III it is seen that the difference between the pd and pp mean multiplicities is consistent with being constant in this energy range, the weighted average of this difference being 0.58 ± 0.05. In a model with vertex factorization, an average of ~1.0 protons emerging from a deuteron target would be expected, compared with the observed ~0.6 protons from a proton target. Therefore, ~0.4 units of the 0.58 units difference can be attributed to protons from the target.

A feature of Table III is that for pd as for[23] pp, the ratio of the mean to the dispersion $\langle N\rangle/D$ is consistent with a constant value of 2.0. To study further the pd distributions and similarities with pp distributions, the normalized moments $C_q = \langle N^q\rangle/\langle N\rangle^q$ were evaluated in the 100–400 GeV/c range.[24] The resulting values are displayed in Fig. 1. The weighted averages at each q and the χ^2 values for the hypotheses that the C_q are energy independent are given in Table IV for pd and for pp (the pn values also given in Table IV are discussed later on). It is apparent that the energy-independent hypotheses are satisfied and also that the pd and pp weighted averages at each q are consistent with being equal. It follows that, in this energy range, pd distributions, like pp distributions[25] are consistent with the Koba-Nielsen-Olesen scaling relation[26]

TABLE III. Properties[a] of *pd* and *pp* multiplicity distributions at 100 to 400 GeV/*c*. $D = (\langle N^2\rangle - \langle N\rangle^2)^{1/2}$, $f_2 = \langle N(N-1)\rangle - \langle N\rangle^2$.

Beam momentum (GeV/*c*)	100 (Ref. 7)	195 (Ref. 13)	200 (Ref. 4)	300 (Ref. 14)	400[a]
$P(pd, N=2)$	0.117 ± 0.010	0.071 ± 0.008	0.071 ± 0.008	0.058 ± 0.011	0.066 ± 0.013
$\langle N\rangle$ *pd*	6.93 ± 0.06	8.30 ± 0.07	8.35 ± 0.06	8.96 ± 0.10	9.49 ± 0.12
$\langle N^2\rangle$ *pd*	59.9 ± 0.9	85.2 ± 1.2	87.1 ± 1.0	99.6 ± 1.9	113.8 ± 2.3
D *pd*	3.45 ± 0.04	4.05 ± 0.04	4.17 ± 0.03	4.39 ± 0.07	4.87 ± 0.07
$\langle N\rangle/D$ *pd*	2.01 ± 0.03	2.05 ± 0.03	2.00 ± 0.02	2.04 ± 0.04	1.95 ± 0.04
f_2 *pd*	5.0 ± 0.3	8.1 ± 0.4	9.0 ± 0.3	10.3 ± 0.6	14.2 ± 0.7
	100 (Refs. 8, 17–19)	205 (Ref. 20)	300 (Ref. 21)	400 (Refs. 8, 22)	
$\langle N\rangle$ *pp*	6.39 ± 0.04	7.67 ± 0.06	8.50 ± 0.09	8.83 ± 0.12	
$\langle N^2\rangle$ *pp*	51.1 ± 0.6	73.5 ± 1.0	90.2 ± 1.5	99.0 ± 1.9	
D *pp*	3.21 ± 0.02	3.82 ± 0.04	4.24 ± 0.06	4.59 ± 0.06	
$\langle N\rangle/D$ *pp*	1.99 ± 0.02	2.01 ± 0.03	2.01 ± 0.04	1.92 ± 0.04	
f_2 *pp*	3.9 ± 0.2	6.9 ± 0.3	9.4 ± 0.5	12.2 ± 0.6	

[a] The contributions of the uncountables' systematic error to the errors are 0.06, 1.6, 0.04, 0.004, and 0.4 for $\langle N\rangle$, $\langle N^2\rangle$, D, $\langle N\rangle/D$, and f_2, respectively.

$$\langle N\rangle \sigma_N/\sigma_a = \psi(N/\langle N\rangle) \quad (4)$$

with the same function ψ.

The above result, that in the 100–400 GeV/*c* energy range *pp* and *pd* multiplicity distributions are consistent with the same function, is rather surprising. Presumably this result does not hold exactly, for that would imply some sort of conspiracy between the presumed contributors to the *pd* distribution of neutron spectator events, pro-

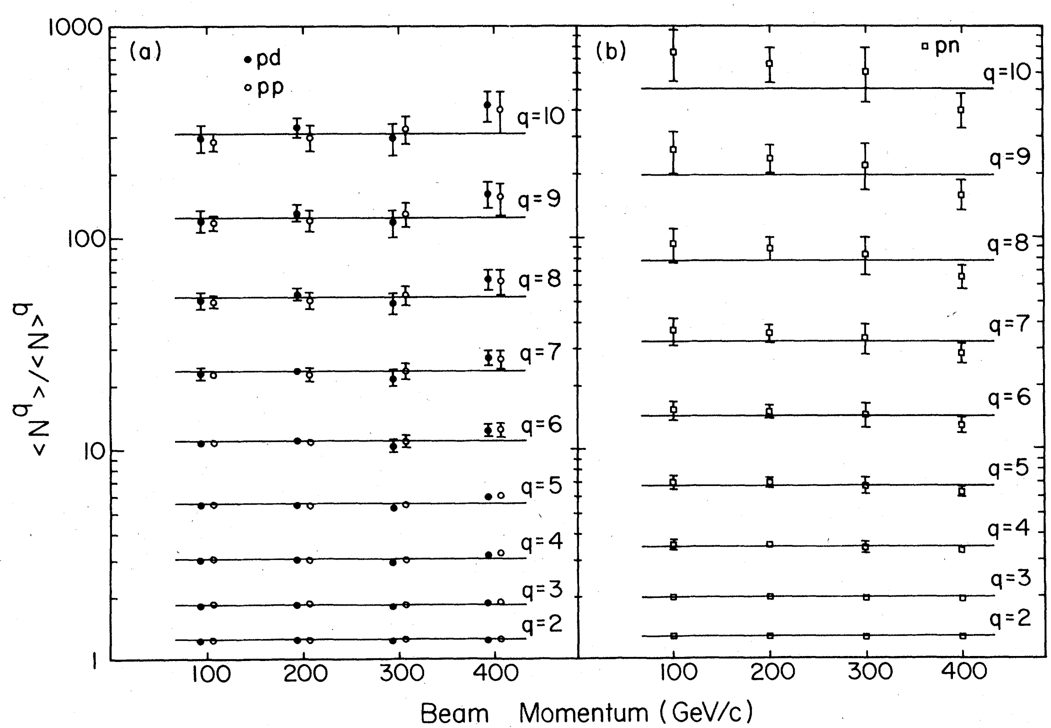

FIG. 1. The normalized moments $\langle N^q\rangle/\langle N\rangle^q$ of the charged-particle multiplicity distributions in *pd*, *pp*, and *pn* interactions in the beam-momentum range 100–400 GeV/*c*. The straight lines are weighted averages for *pd* and *pn*. (Data from Refs. 4, 7, 8, 13, 14, 17–22 and from present experiment).

TABLE IV. Weighted averages of normalized moments $C_q = \langle N^q \rangle / \langle N \rangle^q$ and χ^2 for energy-independence hypothesis (for three degrees of freedom) in the range 100–400 GeV/c.

q	*pd* Average C_q	χ^2	*pp* Average C_q	χ^2	*pn* Average C_q	χ^2
2	1.248 ± 0.004	3.0	1.252 ± 0.004	3.0	1.294 ± 0.007	0.5
3	1.826 ± 0.013	3.3	1.839 ± 0.013	2.9	1.987 ± 0.025	0.5
4	3.02 ± 0.04	3.6	3.05 ± 0.04	2.7	3.48 ± 0.07	0.9
5	5.54 ± 0.10	3.6	5.56 ± 0.10	2.5	6.77 ± 0.21	1.3
6	11.0 ± 0.3	3.6	11.0 ± 0.3	2.2	14.2 ± 0.6	2.3
7	23.6 ± 0.8	3.4	23.2 ± 0.8	2.0	32.5 ± 1.9	2.7
8	54 ± 2	3.2	52 ± 2	1.9	78 ± 6	3.5
9	129 ± 7	3.0	122 ± 7	1.9	198 ±18	4.1
10	325 ±22	2.7	299 ±20	1.9	516 ±57	4.7

ton spectator events, and rescatter events. However, until more accurate data are available, the above serves as a useful mnemonic for describing *pd* multiplicity distributions. The required more accurate data may not be readily forthcoming because of the $N=2$ problem discussed above.

It should be noted that the *pd* distributions studied above do not exclude coherent events, and explicitly include even very slow particles. Thus the comparison above the *pp* distributions is slightly different from heavy-nucleus–hydrogen target comparisons that have been made[27-29] and from that in Ref. 7.

FREE *pn* MULTIPLICITY DISTRIBUTION

The relation between odd-prong distributions in a hadron-deuteron experiment and free hadron-neutron distributions has been discussed in a paper presenting 100-GeV/c results.[7] In the present paper the same assumptions as at 100 GeV/c have been made in order to arrive at 400-GeV/c *pn* multiplicity distributions. Thus a "no-cascade" assumption has been made, and a correction for deuteron-final-state events and for wave-function symmetry requirements has been made. The latter correction, using Eq. (A11) of Ref. 7, assumed the same deuteron final-state cross sections at 400 as at 100 GeV/c, and used values for the recoil deuteron and spectator proton invisibility probabilities of 0.76 and 0.75, respectively, appropriate for the present 5-mm cutoff. The correction, which leads to a mean multiplicity for *pn* interactions that is greater than the odd-prong mean multiplicity by 0.16 units (both for $N \geq 3$), affects only three-prong and five-prong numbers.

To arrive at *pn* topological cross sections, the one-prong cross section was estimated using Eq. (2) and 400-GeV/c *pp* data,[8] and the total inelastic cross section was assumed equal to that for *pp*, with an additional 2% uncertainty. The results are given in Table V and in Fig. 2. Also in Fig. 2, for comparison, are the 400-GeV/c *pp* topological cross sections.[8,22]

TABLE V. *pn* inelastic topological cross sections at 400 GeV/c.

N	$\sigma_N(pn)$ (mb)	Events [a]
1	1.62 ±0.40	
3	4.00 ±0.27	784 ±45
5	4.96 ±0.26	973 ±38
7	5.61 ±0.27	1100 ±34
9	5.29 ±0.26	1037 ±33
11	4.26 ±0.22	835 ±30
13	2.82 ±0.17	553 ±25
15	1.97 ±0.13	387 ±21
17	1.16 ±0.10	227 ±17
19	0.60 ±0.07	118 ±14
21	0.36 ±0.06	70 ±11
23	0.076 ±0.036	15 ± 7
25	0.071 ±0 025	14 ± 5
27	0.015 ±0.015	3 ± 3
29	0.005 ±0.005	1 ± 1
Total	32.8 ±1.2	

[a] See footnote a of Table I.

ENERGY DEPENDENCE OF *pn* MULTIPLICITY DISTRIBUTIONS

In Table VI some low-order moments of *pn* distributions at[4,7,13,14] 100–400 GeV/c are compared. The comparison must be made with some care, because at 195, 200, and 300 GeV/c methods slightly different from the present ones were used to obtain *pn* distributions. At 195 GeV/c the odd-prong plus backward spectator events are assumed to give the *pn* distribution. At 200 and 300 GeV/c the odd-prong events are assumed to give the *pn* distribution (the results of the cascade-model rescatter calculation of Ref. 14 are not used in the present paper). At 195 and 300 GeV/c no correction has been made for either a possible slow-proton-detectability bias or deuteron-

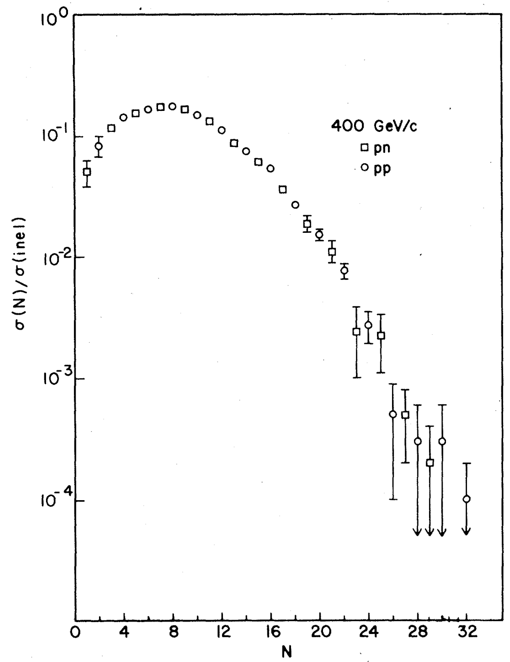

FIG. 2. The charged-particle multiplicity distributions for 400-GeV/*c* *pp* and *pn* inelastic interactions (*pp* data from Refs. 8 and 22).

final-state and wave-function-symmetry effects; however, these two corrections are expected to be small and to some extent cancel each other. At 200 GeV/*c* no correction has been made for deuteron-final-state and wave-function-symmetry effects. At all energies, Eq. (2) is used to estimate the one-prong contribution.

The *pn* mean multiplicities in Table VI give a satisfactory fit ($\chi^2 = 2.7$ for three degrees of freedom) to the relation

$$\langle N\rangle = A + B \ln s \tag{5}$$

with $A = -2.6 \pm 0.7$ and $B = 1.69 \pm 0.11$. In comparison, a similar fit to the *pp* mean multiplicities in Table III gives a satisfactory fit ($\chi^2 = 1.7$ for three degrees of freedom) with $A = -3.2 \pm 0.4$ and $B = 1.83 \pm 0.07$. Within errors, the two B values are equal. That is, the rates of change with energy of the *pn* and the *pp* mean multiplicities are equal, within errors, in this energy range. Equivalently, the difference between the *pn* and *pp* mean multiplicities is consistent with being constant, with a weighted average value of 0.28 ± 0.07.

The data in Table VI show that once again the ratio $\langle N\rangle/D$ is consistent with being constant in this energy range. However, the weighted average value of 1.84 ± 0.02 is significantly lower than the *pp* weighted average of 1.98 ± 0.01.

The normalized moments C_q of the *pn* distributions in the 100–400 GeV/*c* range[24] are shown in Fig. 1(b). Weighted averages, together with the χ^2 values for the hypothesis that each C_q is independent of energy in this range, are given in Table IV. The χ^2 values are satisfactory for the three degrees of freedom. The *pn* average values are significantly different from the *pp* average values. Therefore, while the *pn* data are consistent with KNO scaling, the function ψ in Eq. (4) for *pn* is different from that for *pp*, in the 100–400 GeV/*c* range. However, it is noteworthy in Fig. 1 that at 400 GeV/*c* the *pp* and *pd* C_q values lie above the averaged values, while the *pn* values lie below the averages, such that at each q value the 400-GeV/*c* *pp*, *pn*, and *pd* C_q values are all consistent with being equal. Thus it may be that the functions ψ converge to the same function at higher energies.

The comparison between the *pp* and *pn* multiplicity distributions can be looked at from a slightly different view, as follows. The *pp* and *pn* distributions may be related via a set of equations[7]:

$$\sigma(pn, N+1) = (1 - X_N)\sigma(pp, N) + X_{N+2}\sigma(pp, N+2)\,. \tag{6}$$

The quantity X_N may be interpreted as the prob-

TABLE VI. Comparison of *pn* multiplicity distribution properties at 100 to 400 GeV/*c*. All data come from deuteron-target experiments.

Beam momentum (GeV/*c*)	100 (Ref. 7)	195 (Ref. 13)	200 (Ref. 4)	300 (Ref. 14)	400 [a]
$\langle N\rangle$	6.20 ± 0.11	7.49 ± 0.10	7.36 ± 0.09	7.96 ± 0.15	8.57 ± 0.12
$\langle N^2\rangle$	49.9 ± 1.5	72.9 ± 1.6	70.3 ± 1.3	81.7 ± 3.0	94.8 ± 2.1
D	3.38 ± 0.07	4.09 ± 0.06	4.02 ± 0.06	4.28 ± 0.13	4.63 ± 0.08
$\langle N\rangle/D$	1.83 ± 0.05	1.83 ± 0.04	1.83 ± 0.04	1.86 ± 0.05	1.85 ± 0.04
f_2	5.2 ± 0.5	9.2 ± 0.5	8.8 ± 0.5	10.4 ± 1.0	12.8 ± 0.7
$\langle X_N\rangle$	0.59 ± 0.06	0.59 ± 0.06	0.66 ± 0.05	0.77 ± 0.09	0.63 ± 0.08

[a] The contributions of the uncountables' systematic error to the errors are 0.04, 1.0, 0.03, 0.002, and 0.2 for $\langle N\rangle$, $\langle N^2\rangle$, D, $\langle N\rangle/D$, and f_2, respectively.

ability that a struck proton in an N-prong pp interaction either remains a proton or yields a hyperon–positive-kaon (YK^+) pair. Then similarities or differences between pp and pn distributions can be regarded as following from the X_N values. For example, the mean value of X_N is given by

$$\langle X_N \rangle = 0.5(\langle N \rangle_{pp} - \langle N \rangle_{pn}) + 0.5\,. \quad (7)$$

The resulting $\langle X_N \rangle$ values at 100–400 GeV/c are given in Table VI. The weighted average value of $\langle X_N \rangle$ is 0.64± 0.03, and it is apparent that $\langle X_N \rangle$ is consistent with being constant. The latter result is equivalent to the observation above that the $\langle N \rangle$ values for pp and for pn were consistent with having the same rate of increase as a function of energy.

CONCLUSIONS

The main results and conclusions from this work are as follows:

For 400-GeV/c pd interactions in which particle production occurs, the mean charged-particle multiplicity is 9.49± 0.12 (including slow charged particles).

Comparison of charged-particle multiplicity distributions in pd interactions in the range 100 to 400 GeV/c shows that the ratio of the mean to the dispersion, and the normalized moments, are consistent with the same energy-independent values found for pp interactions at 100–400 GeV/c.

The fraction of 400-GeV/c pd interactions with $N \geq 3$ (N = charged-particle multiplicity) in which rescattering occurs is 0.22± 0.01, a value which is consistent with values found for 100-GeV/c and 200-GeV/c pd interactions.

Multiplicity distributions for 400-GeV/c pn interactions have been obtained, after making a no-cascade assumption and a one-prong estimate. The mean charged-particle multiplicity is 8.57 ± 0.12.

Comparison of pn multiplicity distributions in the range 100 to 400 GeV/c shows that the ratio of the mean to the dispersion, and the normalized moments, are consistent with being independent of energy but have average values that are different from the corresponding pp values. However, at 400 GeV/c the pp and pn normalized moments are not significantly different.

In the 100 to 400 GeV/c range the mean pp multiplicity minus the mean pn multiplicity is consistent with being independent of energy, and has an average value of 0.28± 0.07.

ACKNOWLEDGMENTS

We thank the staffs of the Neutrino Laboratory and 30-inch bubble chamber at Fermilab for their help and cooperation. We thank our scanning and measuring staffs who helped extract these data from the film. This work was supported by the U. S. Department of Energy and the National Science Foundation.

---

*Present address: Technion—Israel Institute of Technology, Haifa, Israel.

†Present address: Lawrence Berkeley Laboratory, Berkeley, California 94720.

‡Present address: Syracuse University, Syracuse, New York 13210.

[1]J. Whitmore, Phys. Rep. 10, 273 (1974).
[2]A. Sheng *et al.*, Phys. Rev. D 11, 1733 (1975).
[3]S. Dado *et al.*, Phys. Lett. 60B, 397 (1976).
[4]T. Dombeck *et al.*, Phys. Rev. D 18, 86 (1978).
[5]J. E. A. Lys *et al.*, Phys. Rev. D. 15, 1857 (1977).
[6]N. W. Dean, Phys. Rev. Lett. 27, 276 (1971).
[7]J. E. A. Lys *et al.*, Phys. Rev. D 16, 3127 (1977).
[8]C. Bromberg *et al.*, Phys. Rev. Lett. 31, 1563 (1973).
[9]Y. Akimov *et al.*, Phys. Rev. Lett. 35, 763 (1975).
[10]Y. Akimov *et al.*, Phys. Rev. Lett. 35, 766 (1975).
[11]R. E. Ansorge *et al.*, Nucl. Phys. B109, 197 (1976).
[12]K. Dziunikowska *et al.*, Phys. Lett. 61B, 316 (1976).
[13]Y. Eisenberg *et al.*, Phys. Lett. 60B, 305 (1976).
[14]A. Sheng *et al.*, Phys. Rev. D 12, 1219 (1975).
[15]J. E. A. Lys, Phys. Rev. D 16, 2181 (1977).
[16]N. W. Dean, Phys. Rev. D 5, 2832 (1972).
[17]J. Erwin *et al.*, Phys. Rev. Lett. 32, 254 (1974).
[18]W. Morse *et al.*, Phys. Rev. D 15, 66 (1977).
[19]A single 100-GeV/c pp multiplicity distribution is obtained by adding the corrected numbers of events at each multiplicity from the three experiments near 100 GeV/c. Moments are then calculated from this single distribution.
[20]S. Barish *et al.*, Phys. Rev. D 9, 2689 (1974).
[21]A. Firestone *et al.*, Phys. Rev. D 10, 2080 (1974).
[22]W. S. Toothacker, University of Michigan Report No. UMBC 77-77, 1977 (unpublished). At each N, numbers of events from Ref. 8 and from this reference were added together to produce the 400 GeV/c pp multiplicity distribution.
[23]P. K. Malhotra, Nucl. Phys. 46, 559 (1963); F. T. Dao, *et al.*, Phys. Lett. 45B, 513 (1973). See also A. Wroblewski, Acta Phys. Pol. B4, 857 (1973).
[24]The multiplicity distributions from the two pd experiments near 200 GeV/c are added together to give a single distribution from which the 200 GeV/c C_q values are calculated.
[25]P. Slattery, Phys. Rev. Lett. 29, 1624 (1972).

[26]Z. Koba *et al.*, Nucl. Phys. B40, 317 (1972).
[27]J. R. Elliott *et al.*, Phys. Rev. Lett. 34, 607 (1975).
[28]P. L. Jain *et al.*, Phys. Rev. Lett. 34, 972 (1975).
[29]W. Busza, in *High Energy Physics and Nuclear Structure—1975*, proceedings of the Sixth International Conference, Santa Fe and Los Alamos, edited by D. E. Nagle *et al.* (AIP, New York, 1975), p. 211.